Computers and Fluids 134–135 (2016) 51–60

Contents lists available at ScienceDirect

Computers and Fluids

journal homepage: www.elsevier.com/locate/compfluid

A note on the dual consistency of the discrete adjoint quasi-one-dimensional Euler equations with cell-centered and cell-vertex central discretizations

Carlos Lozano[a,b,*]

[a] Fluid Dynamics Branch, National Institute for Aerospace Technology (INTA), Carretera de Ajalvir, Km.4, 28850 Torrejón de Ardoz, Spain
[b] Applied Mathematics Department, School of Aerospace Engineering, Technical University of Madrid (UPM), Spain

ARTICLE INFO

Article history:
Received 13 November 2015
Revised 4 April 2016
Accepted 12 May 2016
Available online 13 May 2016

Keywords:
Discrete adjoint equation
Dual consistency
Cell-centered vs. cell-vertex discretization

ABSTRACT

A flow discretization is dual-consistent if the associated discrete adjoint equations are consistent with the analytic adjoint equations. We examine here the formulation and numerical solution of the discrete adjoint quasi-one-dimensional Euler equations derived from a second-order, central-difference, finite volume scheme, for both cell-centered and cell-vertex discretizations. It is shown that, while the cell-vertex discretization is dual-consistent, the cell-centered discretization is not, showing oscillations near the boundaries.

1. Introduction

For some 30 years now, adjoint methods have made its way into Computational Fluid Dynamics and are now being routinely applied to optimal aerodynamic shape design [1–5], error analysis and grid adaptation [6–8], flow stability [9,10] and control [11], among others.

In design applications, the adjoint solution provides the sensitivities of an objective function such as lift or drag with respect to the design variables which parameterize the shape. Such sensitivities can then be used in a gradient-based optimization procedure. In error analysis applications, the adjoint solution provides the sensitivity of the objective function to errors in the flow solution. This information can then be used to obtain a-posteriori error estimates or to perform output-based mesh adaptation.

From a mathematical viewpoint, the (analytic) adjoint equations are derived from the linearized flow equations. For numerical applications, a discretized version of the adjoint equations is required, which can be obtained by discretizing the analytic adjoint equations (the *continuous* approach), or by linearizing the discretized flow equations (the *discrete* approach). As the operations of linearization and discretization do not commute in general, sensitivity derivatives obtained by using the two approaches may not be identical, with discrete adjoint gradients being consistent with finite-difference gradients independently of the mesh size. On the other hand, the continuous adjoint method has the advantage that the adjoint system has a unique formulation which does not depend on the numerical scheme used to solve the flow equations. This approach produces sensitivity derivatives which can be computed with boundary data alone [4], resulting in significant savings, but it is prone to accuracy problems, too [4,12].

However, design or error applications usually focus on the sensitivities and not on the adjoint solutions themselves, partly owing to the lack of exact solutions for the adjoint equations, so there is usually little information concerning the comparison between continuous and discrete adjoint solutions. Furthermore, such comparisons may be inadequate since discrete adjoint solutions are usually plagued with accuracy and consistency issues such as numerical artifacts, layers and oscillations [4,13–16]. These misbehaviors stem from the fact that, for certain discretizations of the flow equations, particularly at the boundaries of the domain, the corresponding discrete adjoint discretization is not dual consistent, that is to say, it is not a consistent discretization of the analytic adjoint equation. Although these matters have no influence on the sensitivities, the lack of consistency has more than aesthetic consequences. In error estimation applications by means of the dual-weighted approach, adjoint solutions must be prolonged from the computational mesh onto an embedded auxiliary mesh obtained by isotropic refinement of the former [17]; hence, inaccuracies in the adjoint solution may affect the prolonged solution rendering it unusable. Likewise, dual consistency improves functional accuracy (including superconvergence properties) as well as the effectiveness of error estimates [16].

* Corresponding author.
E-mail address: lozanorc@inta.es

http://dx.doi.org/10.1016/j.compfluid.2016.05.012
0045-7930/

In this work we focus on the widely used finite-volume, central-differencing discretization with JST dissipation and we apply it to the quasi-one-dimensional Euler equations. We show that on a 1D uniform mesh and for a volume-based cost function (the integrated pressure along the duct), the corresponding discrete adjoint problem is not dual consistent when formulated in a cell-centered approach, while dual consistency is recovered when formulated in a cell-vertex fashion. In earlier analysis (see e.g. [13]), different flux functions were evaluated on the same grid, whereas in this work the flux functions are the same and what changes is actually whether degrees of freedom are located directly on the boundary or not. It is also assessed the extent to what the above conclusion depends on the detailed form of the dissipation, which has been shown to play a crucial role in the consistency of discrete adjoint schemes under different circumstances [18].

This new piece of evidence should add to the long-standing discussions on the relative merits of continuous vs. discrete adjoint approaches on the one hand [19], and cell-centered vs. cell-vertex discretizations [20,21] on the other.

2. Flow equations and discretization

Quasi-1D flows are interesting because, while retaining some of the features of more complex flows (such as shocks), they are nevertheless simple enough to possess exactly computable solutions for both the flow and adjoint equations under very generic circumstances [22].

The quasi-one-dimensional Euler equations for steady flow in a duct of cross-section $h(x)$ on the interval $-1 \le x \le 1$ read [22,23]:

$$R(U,h) = \frac{d}{dx}(hF) - \frac{dh}{dx}P = 0, \tag{1}$$

where

$$U = \begin{pmatrix} \rho \\ \rho u \\ \rho E \end{pmatrix}, \quad F = \begin{pmatrix} \rho u \\ \rho u^2 + p \\ \rho u H \end{pmatrix}, \quad P = \begin{pmatrix} 0 \\ p \\ 0 \end{pmatrix} \tag{2}$$

Here, ρ is the density, u is the velocity, p is the pressure, E is the total energy per unit mass and H is the stagnation enthalpy. It is assumed that the system is closed by the equation of state for an ideal gas

$$p = (\gamma - 1)\rho\left[E - \frac{1}{2}u^2\right], \quad H = E + \frac{p}{\rho} = \frac{\gamma}{\gamma - 1}\frac{p}{\rho} + \frac{1}{2}u^2 \tag{3}$$

where the adiabatic exponent is taken to be $\gamma = 1.4$. If the solution contains a shock at a position x_s, the flow equations must be supplemented with the Rankine–Hugoniot consistency condition

$$[F]_{x_s^-}^{x_s^+} = 0 \tag{4}$$

2.1. Numerical discretization

The flow equations are discretized on a uniform mesh using the central-differencing finite-volume scheme with JST-type artificial dissipation [24] described in [23]. Our conventions for node/cell and face indices are sketched in Fig. 1 below. The main differences between cell-centered and cell-vertex approaches arise at the inlet/outlet boundaries and are summarized in Fig. 2.

For each control volume j of volume (length) Ω_j the solution is obtained by (pseudo)time integration of the equations

$$\Omega_j \frac{dU_j}{dt} + R_j = 0 \tag{5}$$

where, for an interior cell, the numerical residual takes the form

$$R_j = C_{j+\frac{1}{2}} - C_{j-\frac{1}{2}} - \left(D_{j+\frac{1}{2}} - D_{j-\frac{1}{2}}\right) - S_j \tag{6}$$

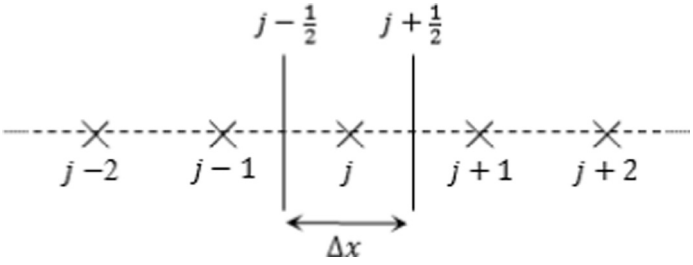

Fig. 1. Scheme of computational mesh.

where

$$C_{j\pm\frac{1}{2}} = \frac{1}{2}h_{j\pm\frac{1}{2}}\left(F_j + F_{j\pm1}\right) \tag{7}$$

is the convective flux at face $j \pm \frac{1}{2}$, $h_{j\pm\frac{1}{2}} \equiv h(x_{j\pm\frac{1}{2}})$ is the duct's cross-section at the face and $F_j = F(U_j)$ is the flux vector (2) evaluated at node/cell j. The artificial dissipation scheme is defined as

$$D_{j-\frac{1}{2}} = h_{j-\frac{1}{2}}\Big(\varepsilon^{(2)}_{j-\frac{1}{2}}\lambda_{j-\frac{1}{2}}(U_j - U_{j-1}) - \varepsilon^{(4)}_{j-\frac{1}{2}}\lambda_{j-\frac{1}{2}}(U_{j+1} - 3U_j + 3U_{j-1} - U_{j-2})\Big) \tag{8}$$

with

$$\begin{aligned} \varepsilon^{(2)}_{j-\frac{1}{2}} &= k_2 \max(\nu_j, \nu_{j-1}), \quad \varepsilon^{(4)}_{j-\frac{1}{2}} = \max(0, k_4 - \varepsilon^{(2)}_{j-\frac{1}{2}}), \\ \nu_j &= \left|\frac{p_{j+1} - 2p_j + p_{j-1}}{p_{j+1} + 2p_j + p_{j-1}}\right|, \\ \lambda_{j-\frac{1}{2}} &= \big((u_j + c_j) + (u_{j-1} + c_{j-1})\big)/2 \end{aligned} \tag{9}$$

where c_j is the speed of sound at node/cell j and $k_2 = 1/2$, $k_4 = 1/64$. Finally, the source term S_j is simply

$$S_j = \begin{pmatrix} 0 \\ p_j \\ 0 \end{pmatrix}\left(h_{j+\frac{1}{2}} - h_{j-\frac{1}{2}}\right). \tag{10}$$

We will consider only subsonic inlet/outlet conditions, which can result in subsonic or shocked transonic flow. Under such conditions, there are two incoming characteristics at the inflow boundary and one incoming characteristic at the outflow boundary. Boundary conditions are then defined by setting $H = H_\infty$ and $p_t = p(1 + \frac{\gamma-1}{2}M^2)^{\frac{\gamma}{\gamma-1}} = p_{t\infty}$ and extrapolating the Mach number $M = u/c$ from the interior at inflow (where $c = \sqrt{\gamma p/\rho}$ is the sound speed), and $p = p_\infty$ (and extrapolating ρ and u) at outflow. In the code, boundary conditions are imposed weakly, details differing between the cell-centered and cell-vertex case:

Inlet

$$\begin{aligned} C_{-\frac{1}{2}} &= h_{-\frac{1}{2}}F(U_{in}), \\ D_{-\frac{1}{2}} &= h_{\frac{1}{2}}\varepsilon^{(2)}_{\frac{1}{2}}\lambda_{\frac{1}{2}}(U_1 - U_0), \\ D_{\frac{1}{2}} &= h_{\frac{1}{2}}\left(\varepsilon^{(2)}_{\frac{1}{2}}\lambda_{\frac{1}{2}}(U_1 - U_0) - \varepsilon^{(4)}_{\frac{1}{2}}\lambda_{\frac{1}{2}}(U_2 - 3U_1 + 3U_0 - U_{-1})\right), \end{aligned} \tag{11}$$

where $U_{-1} = 2U_0 - U_1$ is the value at the ghost node/cell and $U_{in} = U(M_{in}, H_\infty, p_{t\infty})$ (see below for precise definitions). The above choices modify the dissipation scheme at the first two interior mesh cells, reducing the dissipation at the boundary cell, $D_0 = D_{\frac{1}{2}} - D_{-\frac{1}{2}}$, to an undivided second-difference